Journal of Applied Biology & Biotechnology Vol. 11(6), pp. 202-215, Nov-Dec, 2023
Available online at http://www.jabonline.in
DOI: 10.7324/JABB.2023.141954

Novel use of probiotic as acetylcholine esterase inhibitor and a new strategy for activity optimization as a biotherapeutic agent

Abdulrahman M. Qadah[1]*, Amr A. El-Waseif[1], Heba Yehia[2]

[1]Department of Botany and Microbiology, Faculty of Science (Boys), Al-Azhar University, Cairo, Egypt.
[2]Department of Chemistry of Natural and Microbial Products, Pharmaceutical and Drug Industries Research Institute, National Research Centre, Dokki, Giza 12622, Egypt.

ARTICLE INFO

Article history:
Received on: May 26, 2023
Accepted on: September 15, 2023
Available online: October 25, 2023

Key words:
Probiotics,
Acetylcholine esterase inhibitor,
Levilactobacillus brevis,
Alzheimer's disease,
Statistical optimization,
Design of experiment.

ABSTRACT

The communication between the central nervous system and the gastrointestinal organs was first introduced in the 1880s. Further studies followed to ascertain the influence of gut flora on the host`s brain functions, general behavior, and neurodegenerative diseases. Article objectives involved investigate a new promising probiotic as an anti-acetylcholine esterase, and maximize its activity using optimization statistical approaches. Probiotics isolates from different sources underwent anti-acetylcholine esterase activity screening by modified Ellman's method. Where 14 out of the investigated strains showed acetylcholine esterase inhibition (AChEI) activity ranging between 0.407% ± 0.004% for the lowest inhibiting strain (PI22) to 9.846% ± 0.135 for the highest inhibiting strain (PI09). ANOVA analysis and post-ANOVA comparisons showed a significant difference in AChEI% between the tested strains ($P < 0.001$). Taguchi experimental design used to study the effect of each factor and their interactions on the AChEI activity and to enhance the inhibition activity of PI09 strain. ANOVA analysis showed that inoculum size power had a significant effect ($P < 0.05$) on the AChEI%. AChEI% activity for the isolate PI09 was successfully maximized by 60% from 9.846% ± 0.135% to 16.55% ± 0.07%. Finally, the most potent strain (PI09) was identified through 16S rRNA sequencing, aligned using the EZbio database, and identified as *Levilactobacillus brevis*. This is the first report about probiotics activity against acetylcholine esterase results revealed that the screened isolates specially *Levilactobacillus brevis* might have anti-acetylcholine esterase activity, which can allow usage of the probiotics as an auxiliary drug against AD, or to be used for large scale production of AChEIs in the future.

1. INTRODUCTION

Acetylcholine esterase (EC 3.1.1.7, AChE, acetylcholine acetylhydrolase) is a rapid α/β hydrolase whose main function is to terminate the nerve impulse by rapid hydrolysis of the neurotransmitter acetylcholine (ACh) in the synapse and neuromuscular junction. Acetylcholine (ACh) is present in several conducting tissues such as muscles, nerves, peripheral and central tissues, motor and sensory fibers, non-cholinergic and cholinergic fibers, and even in red blood cells [1]. AChE was reported to be encoded by chromosomes 7q22 and 3q26 and its activity was found to be higher in motor than in sensory neurons [2]. The enzyme has different quaternary structures that carry out the same catalytic properties but differ in oligomeric assembly and mode of attachment to the cell surface. It exists a globular homo-oligomers, that is, monomeric G1, dimeric G2, and tetrameric G4, which constitutes the majority of AChEI in the mammalian brain, or asymmetric structures with collagen-like tail, that is, A4, A8, A12 [1,3].

*Corresponding Author:
Abdulrahman M. Qadah,
Department of Botany and Microbiology, Faculty of Science (Boys), Al-Azhar University, Cairo, Egypt.
E-mail: abdulrahman.qadah50 @ gmail.com

Acetylcholine shortage is strongly associated with many disorders including, but not limited to, neuromuscular junction disorders (e.g., myasthenia gravis) and neurodegenerative disorders (e.g., Alzheimer's disease). Myasthenia gravis (MG) is an autoimmune disease associated with the presence of antibodies targeting the acetylcholine receptors [4]. MG is characterized by fluctuating muscle weakness that affects, in particular, the pelvic bones, scapular girdle, axial and bulbar muscles, and it is aggravated with activity [5]. Alzheimer's disease (AD) is a type of irreversible progressive elderly dementia, primarily evident as short-term memory loss, reasoning, and behavioral impairment. It is attributed to changes in cholinergic synaptic gaps on account of ACh levels deficiency through either receptors loss or decreased production by basal forebrain cholinergic neurons [6]. It can be, thus, easily inferred that AChEIs have been efficiently utilized for symptomatic improvement of the aforementioned diseases, for example, pyridostigmine for the former and galantamine, rivastigmine, and donepezil for the latter [6,7].

Acetylcholine esterase inhibitors (AChEIs) obstruct ACh hydrolysis and, therefore, result in its accumulation, longer *in vivo* activity, in addition to hyperstimulation of muscarinic and nicotinic receptors. AChEIs can be classified according to the mode of action into: (1) Irreversible inhibitors

(e.g., organophosphorus compounds), and (2) reversible inhibitors (e.g., galantamine, rivastigmine, and carbamates). By blocking the action of the primary substrate AChE, the inhibitors could be employed in several versatile applications. These applications could be violent such as toxins and chemical warfare agents (e.g., organophosphate toxins, nerve agents, soman, and sarin) that lead to inhibition of AChE in nerve junctions by irreversibly covalently binding to the enzyme inhibitor, leading to muscle paralysis, increased respiratory secretions, respiratory failure, seizures, coma, and death [8]. Peaceful and therapeutic applications also exist, for example, tacrine, rivastigmine, and donepezil that are used in dementia with Lewy bodies patients [9], huperzine A for glaucoma treatment [10], rivastigmine, galantamine, and donepezil for alleviation of AD symptoms [1,11], and neostigmine in the cases of neuromuscular blockade and MG patients [12].

Probiotics are living microorganisms that confer health-improving properties [13]. They include bacteria such as *Bifidobacterium* and *Lactobacillus* and yeasts such as *Saccharomyces.* There are increasing studies that describe how probiotics contribute to improving gut balance by suppressing pathogens and interacting with host cells (e.g., early protection against *Citrobacter rodentium*) [14], accelerating wound healing [15], inhibiting intestinal tumors [16], and improving autism spectrum [17]**.** *Levilactobacillus brevis* was found to produce a wide variety of metabolites naturally as it is the main bacteria in fermented food giving the fermented food its beneficial nature [18]. Many studies refer to *Levilactobacillus brevis* potentials such as antioxidant and immune enhancing activities [19], production of variety of bioactive compounds like γ-aminobutyric acid [20], and β-glucan [21], not to mention the neuroprotective effect of the heat killed cells against oxidative stress [22].

Taguchi experimental designs or robust design methods are statistical designs developed by Genichi Taguchi aiming to enhance the quality of manufactured products, and it was used afterward in many fields such as engineering, biotechnology, and marketing. The Taguchi experimental design assists in improving the process performance by decreasing the noise factors impact [23] while increasing the quality, productivity, and stability. The process conditions can be effectively optimized with a smaller number of experiments using the design of experiments (DOE), where the interactions (noise factors) through the process parameters can be easily determined [24].

This study aimed to investigate and evaluate the capability of the isolated probiotics as promising *in vitro* AChEIs, and therefore, the potential of using them as an auxiliary treatment to alleviate the AD symptoms especially in the early stages of the disease. This was subsequently followed by an attempt to maximize the *in vitro* activity to establish an efficient and economic candidate that could be further employed in large scale production of AChEIs. To the best of the authors' knowledge, this is the first research article to screen and document the probiotics as AChEIs in relation to the neurologic disorder AD.

2. MATERIALS AND METHODS

2.1. Probiotic Strains

Thirty-seven isolates were obtained from cow and buffalo raw milk, yoghurt, and fermented milk. The raw milk samples were obtained from local farms at Al-Daqahliya province and the 6th of October city in Egypt, in May 2021. Raw milk samples were collected in sterile 15 ml falcon tubes while yoghurt and fermented milk were kept in the original packages. All samples were kept at 4°C until analysis. The samples were diluted in the ratio of 1:10 before being quadrant streaked on De Man, Rogosa, and Sharpe (MRS) agar plates and incubated at 37°C for 2 days [25].

2.2. Buffers and Reagents Preparation

2.2.1. Chemicals, reagents, and buffers

All chemicals were of analytical grade, purchased from Sigma Aldrich (St. Louis, MO, USA) and used as received without further purification. Donepezil hydrochloride 5 mg tablets were purchased from a local pharmacy under the trademark of Aricept®, Pfizer©. All solutions were prepared using deionized water of resistivity not less than 18.2 MΩ.cm.

Buffer A: 1 M stock solution of phosphate buffer pH 7.6 was prepared and stored at 4°C and 50 mM working solution was freshly prepared when needed. Buffer B: 1 M stock solution of Tris-HCl pH 7.6 was prepared and stored at 4°C and 50 mM working solution was prepared when needed. Buffer C: Tris-HCl buffer containing 0.1% (v/v) bovine serum albumin (BSA) pH 7.6 was freshly prepared when needed.

Donepezil reference standard (DRS): Donepezil HCl tablets were completely dissolved into 10 ml of methanol 99.8%, each, giving a stock solution with a concentration of 1.2 mM and stored at 4°C, then diluted with buffer B giving a working solution of 0.1 mM concentration.

2.2.2. Acetylcholinesterase Enzyme

Acetylcholine esterase (AChE) (EC 3.1.1.7) from *Electrophorus electricus* (Electrical eel), lyophilized powder, 200-1000 unit/mg protein, and 500 units/vial was purchased from Sigma Aldrich (St. Louis, MO, USA). The lyophilized AChE was dissolved in 5 ml buffer C giving rise to a 100 U/ml stock solution that was preserved at −20°C. Dilutions were prepared when needed using buffer B and sterilized by filtration through 0.45 µm bacterial filter.

2.3. Re-Culturing and Preparation of the Cell Free Filtrate

The strains were refreshed by inoculation into 10 ml MRS broth and incubation for 48 h at 37°C. The tubes were then centrifuged at 5000 RPM for 10 min at 4°C, and the supernatant, designated as cellfree filtrate (CFF), was used for the AChEI assay.

2.4. Acetylcholinesterase Inhibition Assay

The CFF was screened for AChEI through an adaptation of Ellman`s assay using microtiter plates [26,27]**.** The assay was carried out as follows: In a 96-wells microtiter plate, the CFF was mixed with freshly prepared 0.01 U/ml AChE. DRS and galantamine reference standard (GRS), prepared from galantamine hydrobromide and donepezil hydrochloride, were tested, as positive control, under the same conditions. The plate was then incubated at 4°C for 20 min after which 10 µL of 1.5 mM acetylthiocholine iodide (ATCI), 60 µL of freshly prepared 3 mM Ellman's reagent, *5,5'-dithio-bis-(2-nitrobenzoic acid*) (DTNB), and 60 µL of 0.1 M buffer A were immediately added to the wells. The results were measured spectrophotometrically after 3 minutes at 405 nm (BioTek® 800 TS microplate reader, CA, USA). The inhibition was calculated as:

$$\text{AChE Inhibition activity } (\text{AChEI }\%) = \frac{\text{Blank OD-Sample OD}}{\text{Blank OD}} \times 100$$

In case of calculating the AChEI% for standards, Buffer A was used as the blank, while in case of CFF AChEI% calculation MRS was used as the blank.

All experiments were done in triplicates and repeated independently at least 3 times. The results are expressed as mean ± standard deviation.

2.5. Statistical Analysis

All the statistical analyses and design of experiments were performed using Minitab software (Version 19). For all the tests, the level of significance was set for $P \leq 0.05$, two-tailed. Testing for equal variances was performed using Bartlett's method, where the null hypothesis ($P \geq 0.05$) assumes that all variances are equal. Normal distribution was performed using Anderson–Darling and tests as a requirement for ANOVA analysis, where alternative hypothesis ($P \leq 0.05$) assumes that the raw data follow a normal distribution. Finally, ANOVA and post-ANOVA analyses were performed to compare the 27 positive isolates' AChEI activity [28]. ANOVA analysis was carried out using general linear model with Box-Cox transformation using optimal lambda, λ, for the transformation. Equal variances were assumed and alternative hypothesis assumed a significant difference between the AChEI% among all the tested strains. Finally, post-ANOVA analysis was performed using Tukey and Sidak pairwise comparisons to determine the significantly different AChEI% across the individual isolates, where null hypothesis, $P \geq 0.05$ assumed no significant difference between the two isolates, while alternative hypothesis, $P < 0.05$ assumed that there is significant difference between them.

Table 1: The orthogonal array design for 4 factors in different 3 levels.

Factor/Level	Level 1	Level 2	Level 3
pH	4.5	6.2	8
Incubation time (h)	42	44	48
Inoculum size (3.65×10^{n} CFU/mL; *n*=Level)	2	4	6
Enzyme concentration ($\times10^{-3}$ U/mL)	0	15	30

Table 2: The Taguchi design generated using Minitab software (version 19) in L27 (3^4) orthogonal array.

Run #	pH	Incubation time (h)	Inoculum size power ($3.65*10^{n}$ CFU/mL; *n*=level)	Enzyme concentration ($\times10^{-3}$ U/mL)
P01	4	44	6	0
P02	4	44	6	15
P03	4	44	6	30
P04	4	48	4	0
P05	4	48	4	15
P06	4	48	4	30
P07	4	42	2	0
P08	4	42	2	15
P09	4	42	2	30
P10	6	42	4	0
P11	6	42	4	15
P12	6	42	4	30
P13	6	44	2	0
P14	6	44	2	15
P15	6	44	2	30
P16	6	48	6	0
P17	6	48	6	15
P18	6	48	6	30
P19	8	48	2	0
P20	8	48	2	15
P21	8	48	2	30
P22	8	42	6	0
P23	8	42	6	15
P24	8	42	6	30
P25	8	44	4	0
P26	8	44	4	15
P27	8	44	4	30

2.6. Multifactorial Statistical Approaches and AChEi% Activity Enhancement

Four factors in 3 levels were assimilated in L27 (3^4) orthogonal array to study the effects of these factors on the response model (AChEI%). The factors and their levels are summarized in Table 1. Taguchi design of experiment was generated using Minitab software (version 19) and

Table 3: Summarized results of AChEI screening, table showing the mean±SD, variance, and 95% CI for each strain in descending order.

Strain code	Mean±SD	95% CI	V/p**
GRS 0.1mM	**14.969±0.512**	**(14.520, 15.418)**	**NA**
PI09	9.846±0.135	(9.300, 10.392)	0.018
PI35	6.263±0.425	(5.717, 6.809)	0.181
PI24	5.043±0.590	(4.496, 5.589)	0.348
PI03	3.978±2.515	(3.431, 4.524)	6.33
PI01	3.415±0.773	(2.869, 3.961)	0.598
PI37	3.010±0.350	(2.464, 3.556)	0.123
PI14	2.444±1.357	(1.898, 2.990)	1.84
PI11	2.358±0.325	(1.812, 2.904)	0.106
PI19	2.115±0.171	(1.569, 2.661)	0.029
PI23	2.114±0.330	(1.568, 2.660)	0.109
PI08	1.628±0.279	(1.082, 2.174)	0.078
PI07	0.648±0.460	(0.102, 1.194)	0.212
PI05	0.487±0.527	(−0.059, 1.033)	0.277
PI22	0.407±0.004	(−0.139, 0.953)	0
PI02	0±0	(−0.546, 0.546)	0
PI06	0±0	(−0.546, 0.546)	0
PI10	0±0	(−0.546, 0.546)	0
PI15	0±0	(−0.546, 0.546)	0
PI16	0±0	(−0.546, 0.546)	0
PI17	0±0	(−0.546, 0.546)	0
PI25	0±0	(−0.546, 0.546)	0
PI30	0±0	(−0.546, 0.546)	0
PI31	0±0	(−0.546, 0.546)	0
PI32	0±0	(−0.546, 0.546)	0
PI33	0±0	(−0.546, 0.546)	0
PI34	0±0	(−0.546, 0.546)	0
PI36	0±0	(−0.546, 0.546)	0

*Pooled SD=0.615986, **V/p: Variance *P* value

the test runs are shown in Table 2. The 27 runs were tested *in vitro* in four replicates and measured as previously described in AChEI activity assay [29-31].

2.7. Molecular Identification of the Best AChEI Candidate

The DNA of the selected isolate (PI09) was extracted using Wizard genomic DNA purification kit (Promega, Madison, USA). Polymerase chain reaction (PCR) was performed to amplify the 16S ribosomal DNA (Eppendorf Mastercycler® personal thermal cycler) using the primer pair SPO/SP6 targeting the 16S ribosomal DNA regions; StrepF; 5'-AAGAGTTTGATCCTGGCTCAG-3', and StrepR; 5'CTACGGCTACCTTGTTACGA-3' [32]. PCR products were resolved by agarose gel electrophoresis, visualized by ethidium bromide and finally purified by the Microcon YM-100 kit (Bedford, MA, USA). DNA sequencing was done using the Big Dye Terminator V3.0 kit (Thermofisher, USA) through the genetic sequencer (ABI, Foster, USA).

EZBioCloud database (https://www.ezbiocloud.net) was used to retrieve the closest related sequences and MEGA 11 software was used to align the sequences and construct the neighbor-joining (NJ) phylogenetic tree that demonstrates evolutionary relatedness of the strains through the p-distance method and 1000 bootstrap replications for each cluster [33-36].

Table 4: Summarized means of AChEI%±SD for standards.

Reference STD	Mean±SD	95% CI
Donepezil 0.1 mM	12.284±0.374	(11.836, 12.733)
Galantamine HBr 0.1 mM	14.969±0.512	(14.520, 15.418)
Galantamine HBr 0.01 mM	13.749±0.519	(13.300, 14.197)
Galantamine HBr 0.001 mM	12.634±0.673	(12.185, 13.083)
Galantamine HBr 0.0001 mM	11.96±0.176	(11.512, 12.409)

*Pooled SD=0.4808

Table 5: Coefficients for transformed response compared to the SE coefficient and the model coefficient.

Term	Coef	SE Coef	t-value	*P*-value
Constant	−10.016	0.240	−41.69	0.000
Isolate ID				
PI01	11.22	1.22	9.16	0.000
PI02	−10.71	1.22	−8.74	0.000
PI03	11.16	1.22	9.11	0.000
PI05	1.54	1.22	1.26	0.210
PI06	−10.71	1.22	−8.74	0.000
PI07	5.65	1.22	4.61	0.000
PI08	10.49	1.22	8.56	0.000
PI09	12.30	1.22	10.04	0.000
PI10	−10.71	1.22	−8.74	0.000
PI11	10.87	1.22	8.87	0.000
PI14	10.74	1.22	8.77	0.000
PI15	−10.71	1.22	−8.74	0.000
PI16	−10.71	1.22	−8.74	0.000
PI17	−10.71	1.22	−8.74	0.000
PI19	10.76	1.22	8.79	0.000
PI22	9.12	1.22	7.44	0.000
PI23	10.75	1.22	8.78	0.000
PI24	11.63	1.22	9.49	0.000
PI25	−10.71	1.22	−8.74	0.000
PI30	−10.71	1.22	−8.74	0.000
PI31	−10.71	1.22	−8.74	0.000
PI32	−10.71	1.22	−8.74	0.000
PI33	−10.71	1.22	−8.74	0.000
PI34	−10.71	1.22	−8.74	0.000
PI35	11.85	1.22	9.67	0.000
PI36	−10.71	1.22	−8.74	0.000

*VIF=1.93 for all strains

3. RESULTS

3.1. Isolated Probiotic Strains Characteristics

Twenty-seven out of the 37 isolated strains were found to meet the macroscopic, microscopic, and oxygen requirements characteristics of the Lactobacillaceae, and Bifidobacteriaceae families.

3.2. ACHEI% of the Tested Isolates

PI09 exhibited the most potent AChEI% among the tested strains (9.89 ± 0.16), followed by PI35 and PI24 with AChEI% of 6.23 ± 0.56 and 5.01 ± 0.81, respectively [Table 3 and Figure 1]. The standard donepezil (0.1 mM) inhibited AChE activity by 12.327% ± 0.521, while galantamine's potential varied according to the concentration where the highest tested concentration (0.1 mM) showed 15.036% ± 0.691 inhibition [Table 4].

3.3. Statistical Analysis

Statistical general linear model ANOVA was performed using optimal lambda λ for the Box-Cox transformation as the null hypothesis is rejected; thus, the raw data does not follow the normal distribution in Anderson–Darling normality measures [Figure 2]. The Box-Cox method estimated the rounded lambda equal to 0.010894 and zero (95% CI of −0.0166060, 0.0383940). ANOVA analysis showed a statistically significant difference in AChEI% between the 27 isolated strains (F-value $_{(108,134)}$ = 73.65, $P < 0.001$). Model and SE coefficients comparing the isolates are illustrated in Table 5 where the results also reflected the tests' precision and accuracy; model R^2 = 96.66% and adjusted R^2 =93.38%.

Statically significant differences between the isolated strains' AChEI% were determined using Sidak and Tukey pairwise (HSD Post-HOC analysis). Grouping results are summarized in Table 6, where it was found that "PI09" was the most significantly different from the other strains. Tables 1 and 2 in appendix 1 showing significant and insignificant differences in means between groups with the 95% CI for each.

3.4. Maximizing the Inhibition Activity for the Most Potent Strain

In this study, the aim was to maximize the AChEI% for the most potent strain (PI09) using orthogonal array (Taguchi Model) by optimizing the production conditions. Taguchi design runs, responses, mean, and design

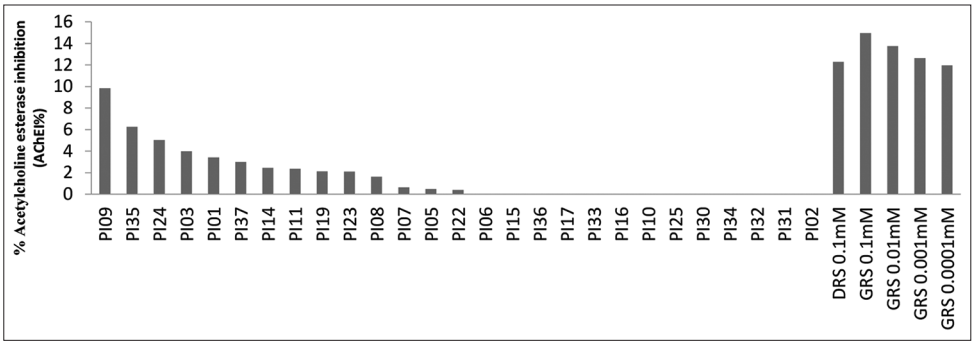

Figure 1: Inhibition of acetylcholine esterase activity by isolated probiotics versus different concentrations of GRS and DRS.

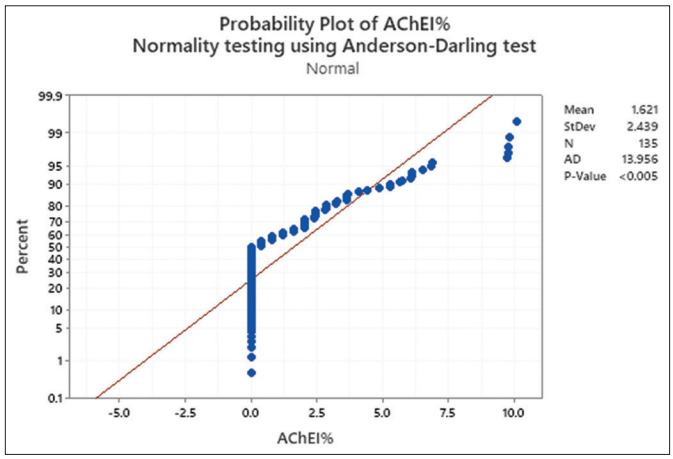

Figure 2: Anderson–Darling test results for normality, $P < 0.05$.

predicted values are depicted in Table 7. The experimental results for each run, compared to the model-predicted mean, are shown in Figure 3. The prediction error was calculated from the following equation:

Mean squared error (MSE) = $(1/n \sum \hat{Y}-)^2$

= $1/n \sum R^2$; R=Residuals

= 1/27 (0.0081) = 0.0003 %

Acceptance criteria not more than (NMT) 15%.

3.5. Signal to Noise Ratio (S/N Ratio or SNR)

This study aimed to increase the AChEI% activity while using pH, temperature, inoculum size, and the enzyme concentration as the control factors at three levels. These control factors values were used to calculate the corresponding S/N ratio using the following equation:

$$S/N = -10 \log(\sum \frac{1}{y^2}) / n)$$

"y:" response factor, "n:" number of tests.

Samples S/N ratio means were calculated at each run conditions then the effect of the individual control factor on S/N ratio was obtained. The higher the S/N ratio (SNR), the better the effect. Thus, from Table 8, it can be concluded that the most effective control factor on the SNR is the inoculum size at level 3 (inoculum power of 6) with SNR 22.02, followed by enzyme concentration at level 2 (15×10^{-3} U/ml) with SNR of −32.24, then pH at level 1 (pH 4) with SNR of −55.99.

Table 6: Post-ANOVA Tukey and Sidak pairwise comparison for the isolates, using grouping and 95% CI.

Isolate ID	Mean	Tukey Grouping				Sidak Grouping		
PI09	9.84567	A				A		
PI35	6.25185	A				A		
PI24	5.01300	A				A		
PI01	3.34355	A				A		
PI03	3.14389	A	B			A		
PI37	2.99241	A	B			A		
PI11	2.34036	A	B			A		
PI19	2.10951	A	B			A		
PI23	2.09235+	A	B			A		
PI14	2.06779	A	B			A		
PI08	1.60802	A	B			A		
PI22	0.40692	A	B			A		
PI07	0.07988		B	C		A	B	
PI05	0.00834			C			B	
PI17	0.00000				D			C
PI31	0.00000				D			C
PI06	0.00000				D			C
PI10	0.00000				D			C
PI25	0.00000				D			C
PI30	0.00000				D			C
PI32	0.00000				D			C
PI33	0.00000				D			C
PI34	0.00000				D			C
PI36	0.00000				D			C
PI15	0.00000				D			C
PI16	0.00000				D			C
PI02	0.00000				D			C

*Means that do not share a letter are significantly different. **Number of replicates *n*=5

The least effective factor, on the other hand, was incubation time at level 2 (44 h) with SNR of −77.94. Figure 4 depicts the main effects, through the SNR, according to the Taguchi model. Thus, the optimized experimental design that should theoretically result in the highest AChEI% is: pH 4, inoculum power of 6, incubation time = 44 h, and enzyme concentration of 15 x 10^{-3} U/ml. The actual value for the

Table 7: Summarized results of experimental runs and the model-predicted values.

Run #	Response 1	Response 2	Response 3	Response 4	Mean	Standard deviation	Predicted values	Residuals
P01	12.17	13.04	13.15	12.17	12.63	0.54	13.29	−0.66
P02	11.30	12.17	11.40	11.30	11.54	0.42	13.70	−2.16
P03	6.95	8.69	8.77	6.95	7.84	1.03	10.22	−2.38
P04	0.00	0.00	0.00	0.00	0.00	0.00	1.31	−1.31
P05	4.34	5.21	4.38	4.34	4.57	0.43	5.49	−0.92
P06	4.34	5.21	4.38	4.34	4.57	0.43	2.52	2.05
P07	0.00	0.00	0.00	0.00	0.00	0.00	−1.96	1.96
P08	2.60	3.47	2.63	2.60	2.83	0.43	−0.24	3.07
P09	0.00	0.00	0.00	0.00	0.00	0.00	−0.31	0.31
P10	0.00	0.00	0.00	0.00	0.00	0.00	0.65	−0.65
P11	0.86	0.86	0.87	0.86	0.87	0.00	3.03	−2.16
P12	0.00	0.00	0.00	0.00	0.00	0.00	2.37	−2.37
P13	0.00	0.00	0.00	0.00	0.00	0.00	1.31	−1.31
P14	0.00	0.00	0.87	0.00	0.21	0.44	1.14	−0.93
P15	0.00	0.00	0.00	0.00	0.00	0.00	−2.06	2.06
P16	14.78	15.65	15.78	14.78	15.25	0.54	13.29	1.96
P17	14.78	15.65	14.91	14.78	15.03	0.42	11.96	3.07
P18	15.65	16.52	15.78	15.65	15.90	0.42	15.59	0.31
P19	0.00	0.00	0.00	0.00	0.00	0.00	0.65	−0.65
P20	0.00	0.00	0.00	0.00	0.00	0.00	2.15	−2.15
P21	0.00	0.00	0.00	0.00	0.00	0.00	2.37	−2.37
P22	10.43	11.30	10.52	10.43	10.67	0.42	11.98	−1.31
P23	11.30	11.30	11.40	11.30	11.32	0.05	12.25	−0.93
P24	16.52	16.52	16.66	16.52	16.55	0.07	14.50	2.05
P25	5.21	5.21	5.26	5.21	5.22	0.02	3.27	1.95
P26	10.43	10.43	9.64	10.43	10.23	0.39	7.16	3.07
P27	0.00	0.00	0.00	0.00	0.00	0.00	−0.31	0.31

*Calculated prediction error from the table=0.0003%, Accepted criteria<15%

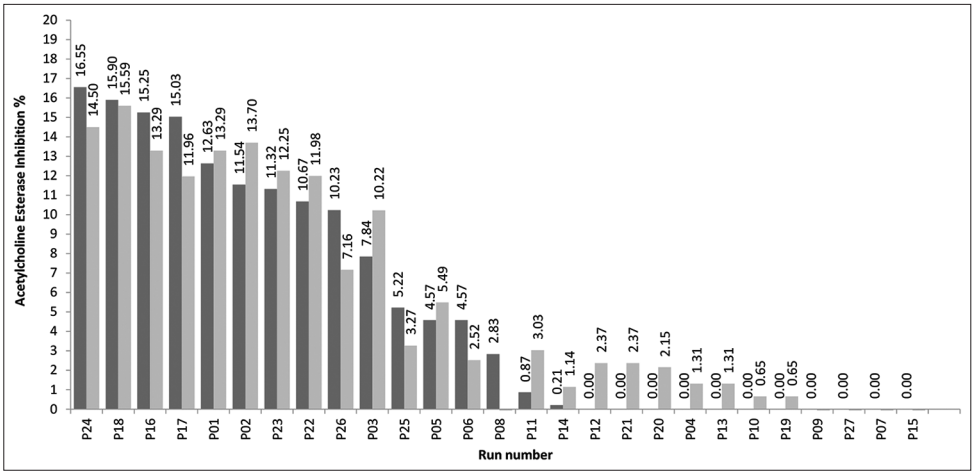

Figure 3: Experimental (actual) results compared to the model-predicted mean for each run.

design SNR was found to be 21.23 while the predicted was 48.98.

The SNR for the interaction between the aforementioned control factors affecting the AChEI% was also determined, where none of the interactions was found to have significant effect ($p > 0.05$) on the AChEI% SNR. However, the interaction between incubation time and enzyme concentration was found to have the highest SNR (SNR = 9.5) at 42 h and 15 × 10^{-3} U/ml, followed by the interaction between inoculum size power and enzyme concentration (SNR = 22.04) at

6 power and 15 × 10^{-3} U/ml, then the interaction between pH and enzyme concentration (SNR = 14.40) at pH 4 and 15 × 10^{-3} U/ml [Figure 5].

3.6. Model Significance and ANOVA for SNR

Model significance was determined by calculating R^2 and adjusted R^2. The calculated values were 89.86% and 56.05%, respectively. ANOVA analysis was performed to recognize the most significant factors affecting the AChEI% activity and to calculate the error caused by the uncontrollable factors that are not included in the experiment. Table 9 shows the calculated ANOVA for the control factors and interactions between these factors affecting the SNR of AChEI%. Only the inoculum size power was found to have a significant effect on the AChEI% SNR with $P = 0.004$.

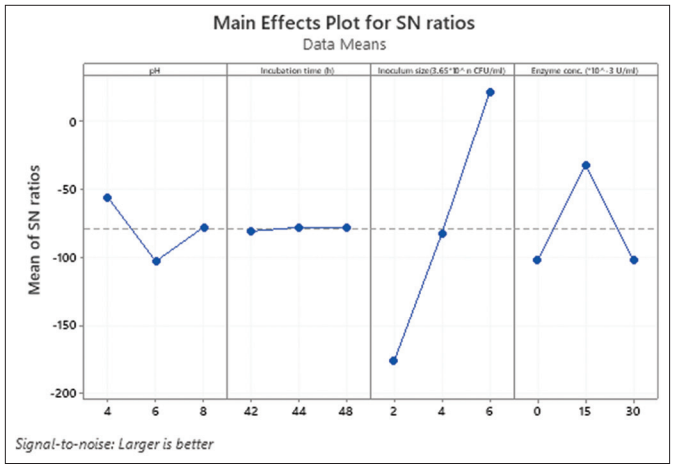

Figure 4: Main effects plot for SNR, showing the best AChEI% SNR at pH 4, incubation time (44 h), inoculum size power of 6, and enzyme concentration of 0.015 U/ml.

3.7. Means Optimization

In Table 10, the influence of each control factor on the AChEI% is shown. The larger the value, the higher the response. Thus, it was found that the most affecting factors are the inoculum size power at level 3 (Inoculum size power = 6) with a mean of 12.63, followed by the incubation time at level 3 (48 h) with a mean of 6.14, then the enzyme concentration at level 2 (15 × 10^{-3} U/ml) with a mean of 6.29, and, finally, the pH at level 3 (pH 8) with a mean of 6.00. By applying these optimized conditions, the AChEI% was predicted at 15.27, while the best experimental value was 15.9 [Figure 6], noting that the model's predicted value has no parallel experimental result as it was not generated in the Taguchi design used in this study.

Interactions between the control factors affecting means were also determined [Figure 7]. The interaction between enzyme concentration, pH, inoculum size power, and incubation time was investigated and none of them was found to have a significant effect ($P > 0.05$). The interaction between pH and enzyme concentration, however, was found to produce the highest value (7.18) at pH 8 and enzyme concentration of 0.015 U/ml, followed by the interaction between enzyme concentration and incubation time (mean = 7.33) and that between enzyme concentration and inoculum size power (mean = 13.43).

Model significance was determined by calculating R^2 and adjusted R^2, where the calculated values were found to be 90.58% and 59.18%, respectively. Table 11 shows the calculated ANOVA for the factors influencing the AChEI% and the interactions between them. Only the inoculum size power was found to have a significant effect on the

Table 8: Response table for S/N ratio (SNR).

Level	pH	Incubation time (h)	Inoculum size power (3.65*10^n CFU/mL)	Enzyme conc. (*10^{-3} U/mL)
1	**−55.99**	−80.70	−176.46	−102.16
2	−103.00	**−77.94**	−82.26	**−32.24**
3	−77.71	−78.06	**22.02**	−102.30
Delta	47.01	2.76	198.48	70.06
Rank	3	4	1	2
Seq SS	9963	44	177431	29392
Contribution%	3.15	0.013	56.12	9.29

*Larger S/N ratio is better, Bold values are the highest S/N ratio values

Table 9: Analysis of variance for SN ratios.

Source	DF	Seq SS	Adj SS	Adj MS	F-value	*P*-value
pH	2	9963	9963	4981.3	0.93	0.444
Incubation time	2	44	44	22.0	0.00	0.996
Inoculum size power	2	177431	177431	88715.6	16.60	0.004
Enzyme conc.	2	29392	29392	14696.2	2.75	0.142
pH*Enzyme conc.	4	19358	19358	4839.4	0.91	0.516
Incubation time *Enzyme conc.	4	28427	28427	7106.7	1.33	0.359
Inoculum size power *Enzyme conc.	4	19480	19480	4870.0	0.91	0.514
Residual error	6	32069	32069	5344.8		
Total	26	316163				

Incubation time (h), Inoculum size power (3.65*10^n CFU/mL), and Enzyme conc. (*10^{-3} U/mL).

Table 10: Response table for means.

Level	pH	Incubation time (h)	Inoculum size power ($3.65*10^n$ CFU/mL)	Enzyme conc. ($*10^{-3}$ U/mL)
1	4.8900	4.6962	0.3390	4.8659
2	5.2532	5.3017	2.8320	6.2938
3	6.0033	6.1486	12.9755	4.9869
Delta	1.1132	1.4525	12.6365	1.4279
Rank	4	2	1	3
Seq SS	5.801	9.581	806.353	11.284
Contribution%	0.58	0.97	82.00	1.14

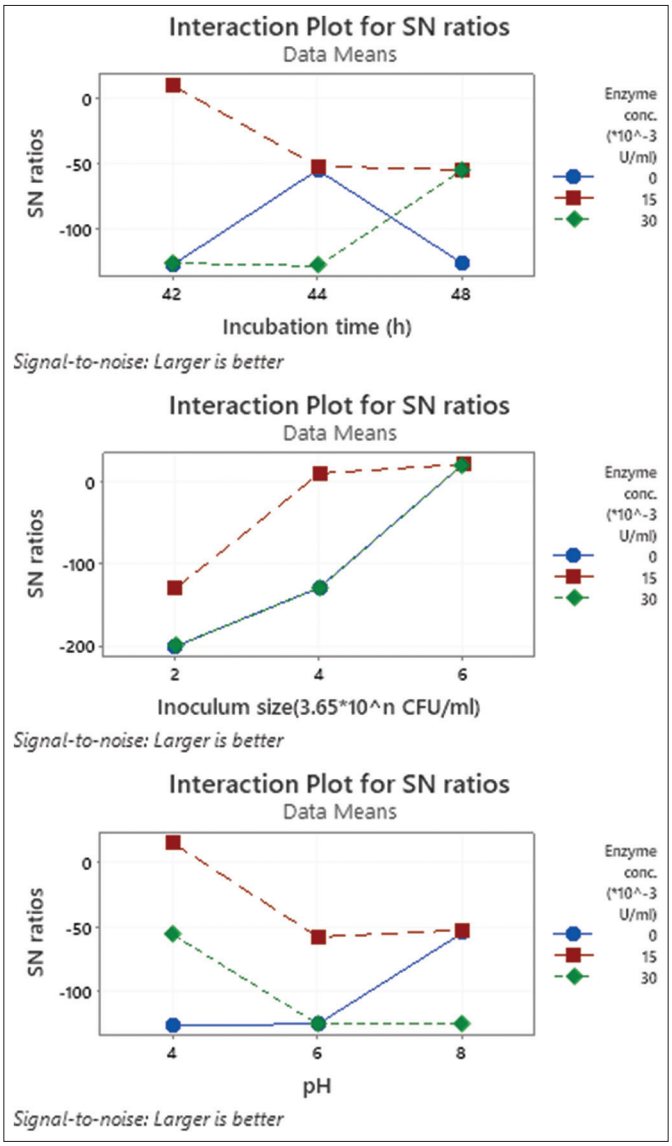

Figure 5: Interaction plots for SNR, showing the interaction between the control factors and its impact on the AChEI% SNR.

AChEI% with p-value of 0.001.

3.8. Contour and Surface Plots

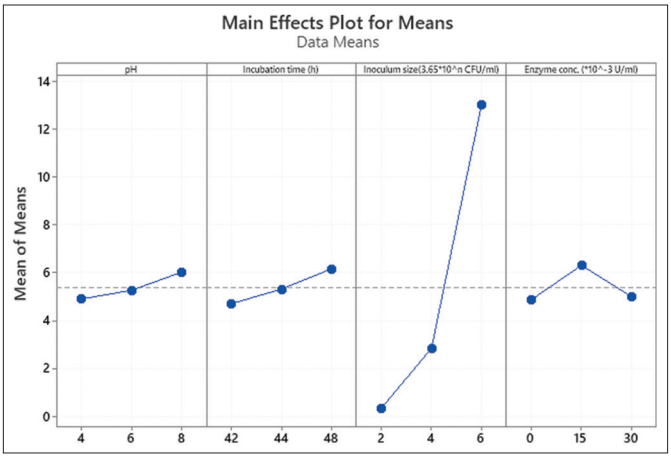

Figure 6: Main effects plot for factors means, showing the best AChEI% Means at pH 8, incubation time of 48 h, inoculum size power of 6, and enzyme concentration of 0.015 U/ml.

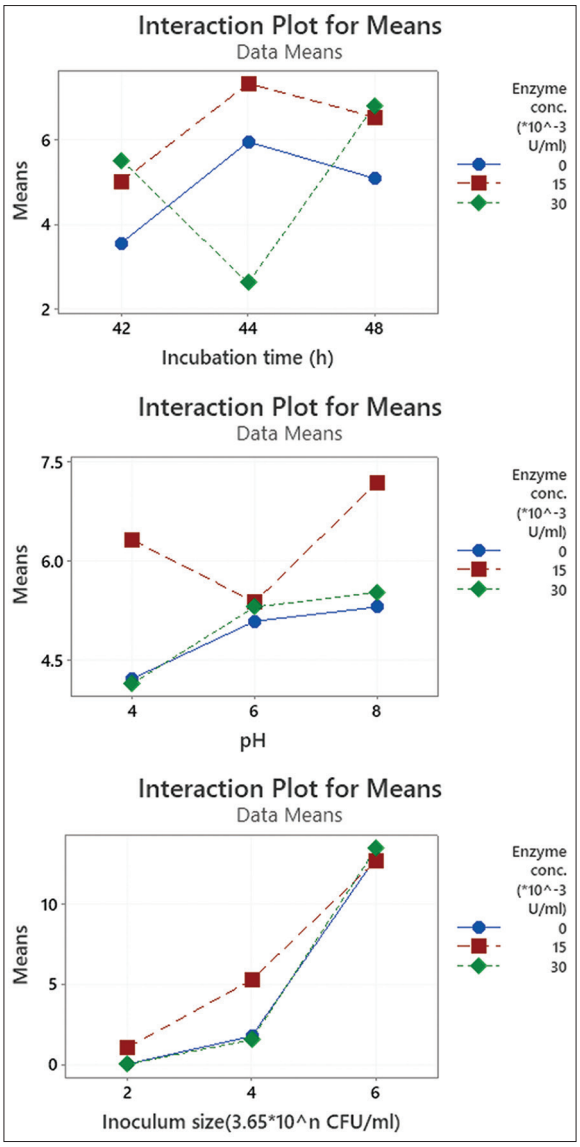

Figure 7: Interaction plots for means, showing the interaction between the different factors and its impact on the AChEI%.

Table 11: Analysis of variance for means.

Source	DF	Seq SS	Adj SS	Adj MS	F-value	*P*-value
pH	2	5.801	5.801	2.901	0.19	0.833
Incubation time	2	9.581	9.581	4.790	0.31	0.744
Inoculum size power	2	806.353	806.353	403.177	26.12	0.001
Enzyme conc.	2	11.284	11.284	5.642	0.37	0.708
pH*Enzyme conc.	4	4.433	4.433	1.108	0.07	0.988
Incubation time * Enzyme conc.	4	35.493	35.493	8.873	0.57	0.692
Inoculum size power * Enzyme conc.	4	17.718	17.718	4.430	0.29	0.876
Residual error	6	92.622	92.622	15.437		
Total	26	983.285				

Incubation time (h), Inoculum size power ($3.65*10^n$ CFU/mL), and Enzyme conc. ($*10^{-3}$ U/mL)

Table 12: Regression model equation verification against the actual values, where R stands for the residuals.

Run No.	Experimental value	Predicted value	R*	R^2
P1	12.64	10.90	1.74	3.01
P2	11.55	10.99	0.56	0.31
P3	7.85	11.07	−3.22	10.39
P4	0.00	5.38	−5.38	28.94
P5	4.57	5.62	−1.04	1.09
P6	4.57	5.86	−1.28	1.64
P7	0.00	−1.77	1.77	3.13
P8	2.83	−2.13	4.96	24.59
P9	0.00	−2.48	2.48	6.17
P10	0.00	4.89	−4.89	23.89
P11	0.87	4.75	−3.88	15.03
P12	0.00	4.61	−4.61	21.24
P13	0.00	−0.96	0.96	0.92
P14	0.22	−1.09	1.31	1.73
P15	0.00	−1.23	1.23	1.51
P16	15.25	12.04	3.22	10.34
P17	15.03	12.49	2.54	6.45
P18	15.90	12.95	2.95	8.73
P19	0.00	0.17	−0.17	0.03
P20	0.00	0.41	−0.41	0.17
P21	0.00	0.65	−0.65	0.42
P22	10.68	11.55	−0.87	0.76
P23	11.33	11.62	−0.29	0.09
P24	16.56	11.70	4.86	23.59
P25	5.23	5.70	−0.47	0.22
P26	10.24	5.78	4.46	19.87
P27	0.00	5.86	−5.86	34.38
Total	145.32	145.32	0.00	248.64

*Calculated prediction error = 9.208%, acceptance criteria < 15%

To determine the effect of the interaction between the studied factors on AChEI%, in both the model predicted values and the actual values, contour and surface plots were analyzed [Figures 8-12].

3.9. Regression Model

Fitted regression model was performed to fit the experimental data and to identify the parallel terms of the model. The obtained fitted regression equation was:

Means = −15.7 + 0.242 [pH] + 0.163 [Incubation time (h)] + 3.086 [Inoculum size power ($3.65*10^n$ CFU/ml)] - 0.25 [Enzyme conc. ($*10^{-3}$ U/ml)] + 0.0024 [pH*Enzyme conc. ($*10^{-3}$ U/ml)] + 0.0050 [Incubation time (h) * Enzyme conc. ($*10^{-3}$ U/ml)] + 0.0048 [Inoculum size power ($3.65*10^n$ CFU/ml) * Enzyme conc. ($*10^{-3}$ U/ml)]

Verification experiment was carried out to verify the model accuracy [Table 12]. The prediction error was calculated from the following equation:

$$MSE=\frac{1}{n}\sum(\hat{Y}-Y)^2=\frac{1}{n}\sum R^2;\ R=\text{Residuals}=\frac{1}{27}(248.64)$$

$$=9.208843\%$$

$$=1/27\ (248.64)=9.208843\ \%$$

The calculated prediction error was found to be 9.2088%, which did not exceed 15%. Thus, the model could be verified to accurately predict the AChEI% at different settings.

Finally, AChEI% was successfully maximized by 60% from 9.84% to 16.55 after the Taguchi optimization. The Pareto chart of the standardized effect for each term and its interactions prove that only the inoculum size power had the utmost significant effect on the AChEI% [Figure 13].

3.10. Molecular Identification of the Most Potent Isolate

The most active AChEI candidate (PI09) was identified according to its 16S rDNA gene sequence and comparing it to the closest related strains [Figure 14]. The isolate, hence, showed highest similarity (65.73%) to *Levilactobacillus brevis* ATCC 14869 and was deposited in the GenBank® under the accession number KI271266.

4. DISCUSSION

Probiotics are commensal microorganisms, providing safe and cheap auxiliary substances for therapeutic use alleviating different disease symptoms, for example, Inflammatory bowel disease IBD [37], *Helicobacter pylori* infection [38], and colorectal cancer [39]. The previous studies highlighted the ability of the probiotics to affect the brain through the microbiota-gut-brain axis [40]. In this context,

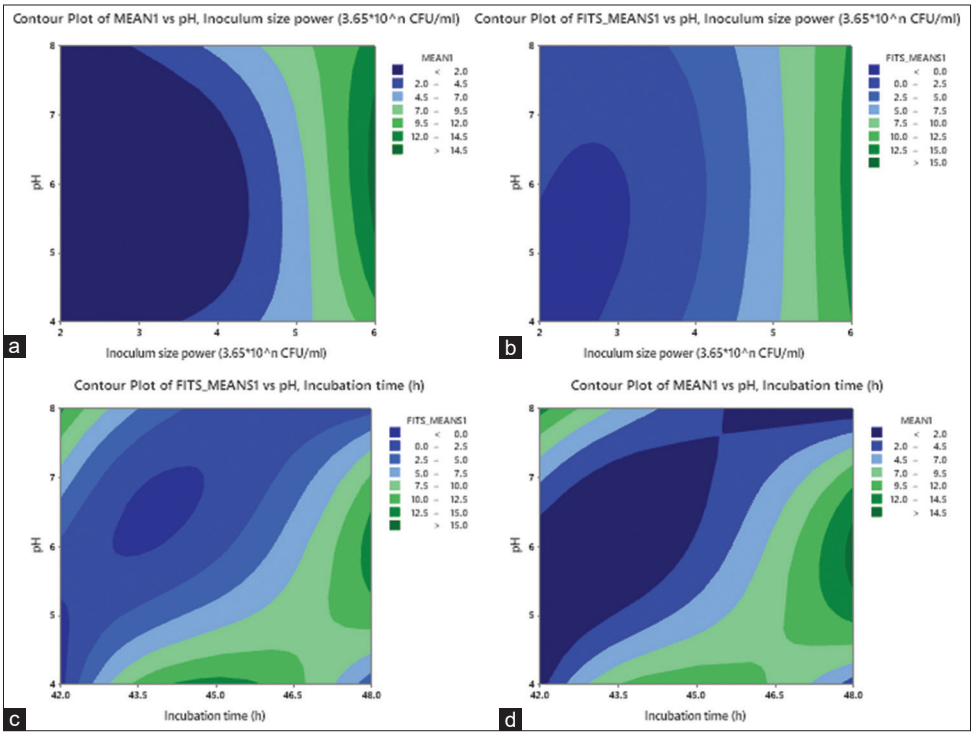

Figure 8: Contour plot of model-predicted values (Fits_means1) and experimental values (Mean1) for pH and inoculum size power (a and b) and pH and incubation time (c and d).

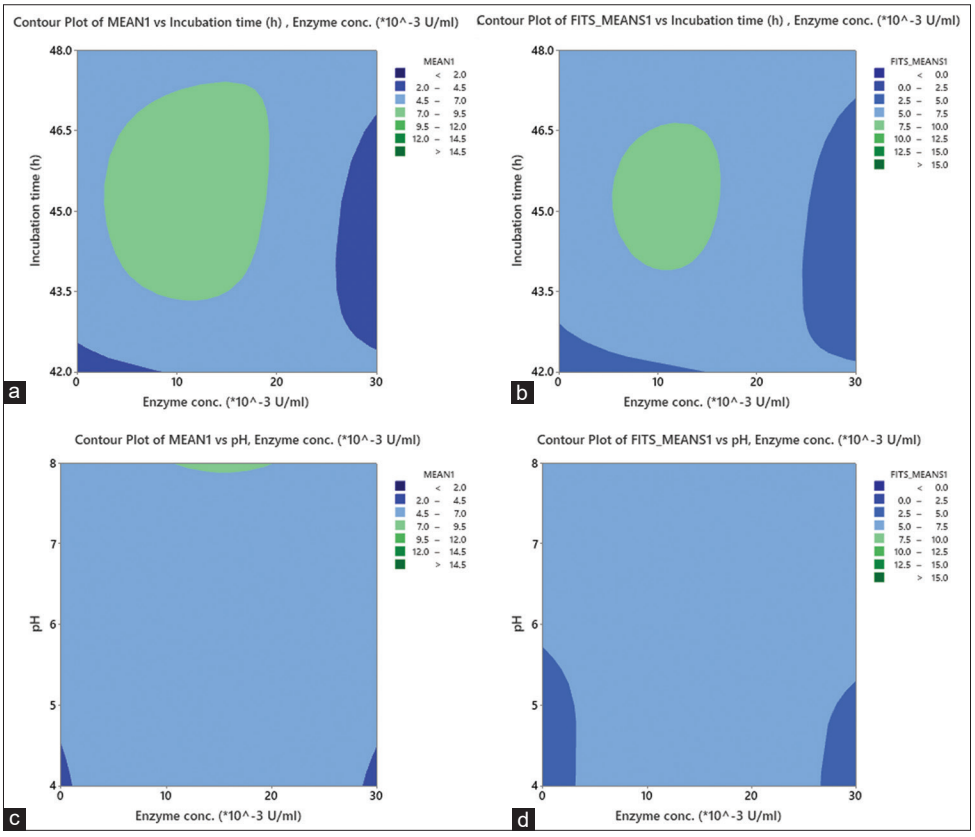

Figure 9: Contour plot of model-predicted values (Fits_means1) and experimental values (Mean1) for incubation time and enzyme concentration (a and b) and pH, and enzyme concentration (c and d).

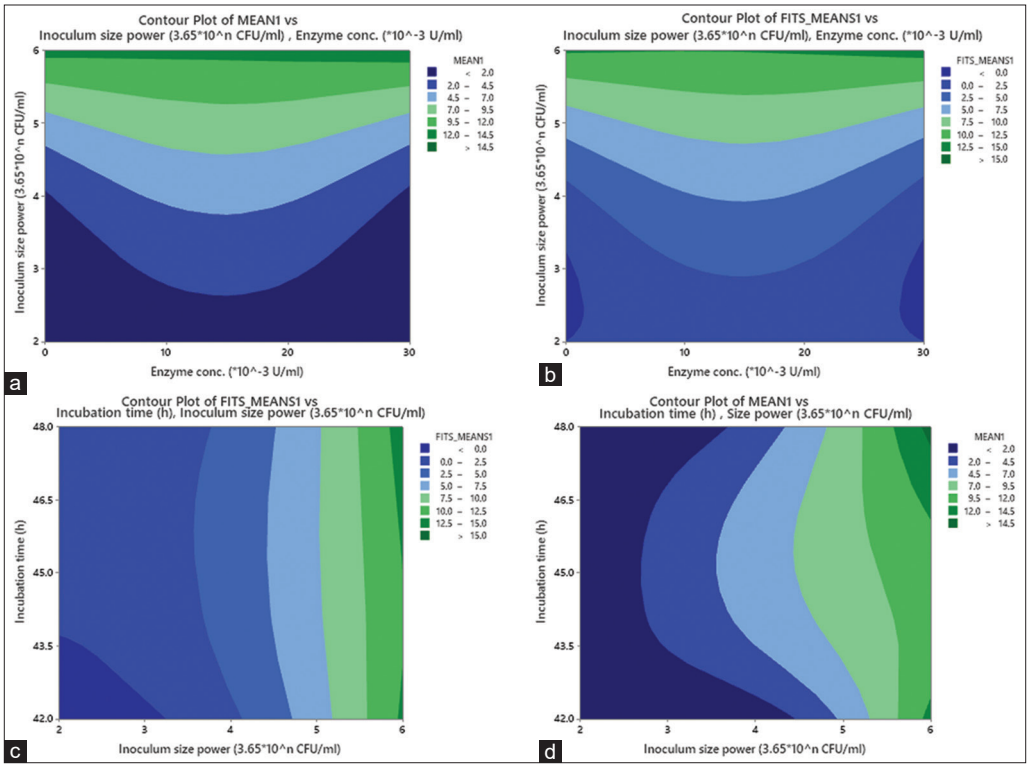

Figure 10: Contour plot of model-predicted values (Fits_means1) and experiment a values (Mean1) for inoculum size power and enzyme concentration (a and b) and incubation time and inoculum size power (c and d).

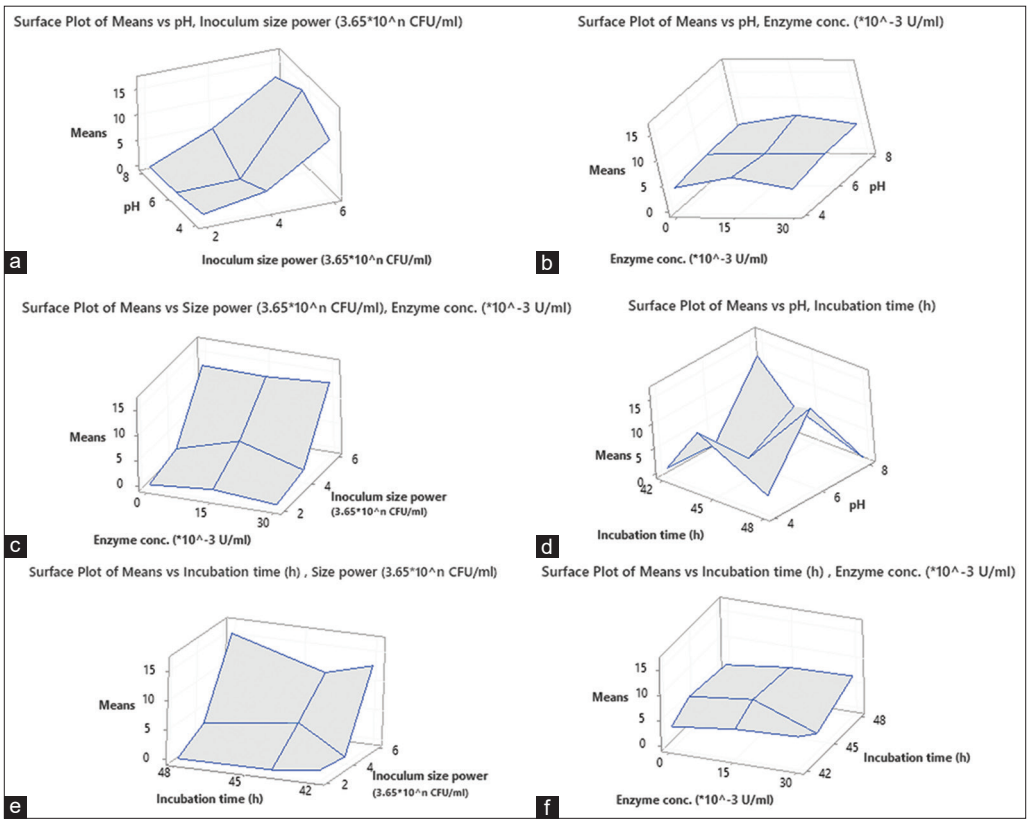

Figure 11: Surface plot of actual means (Means) for (a) inoculum size power and pH, (b) pH and enzyme concentration, (c) inoculum size power and enzyme concentration, (d) pH and incubation time, (e) inoculum size power and incubation time, and (f) incubation time and enzyme concentration.

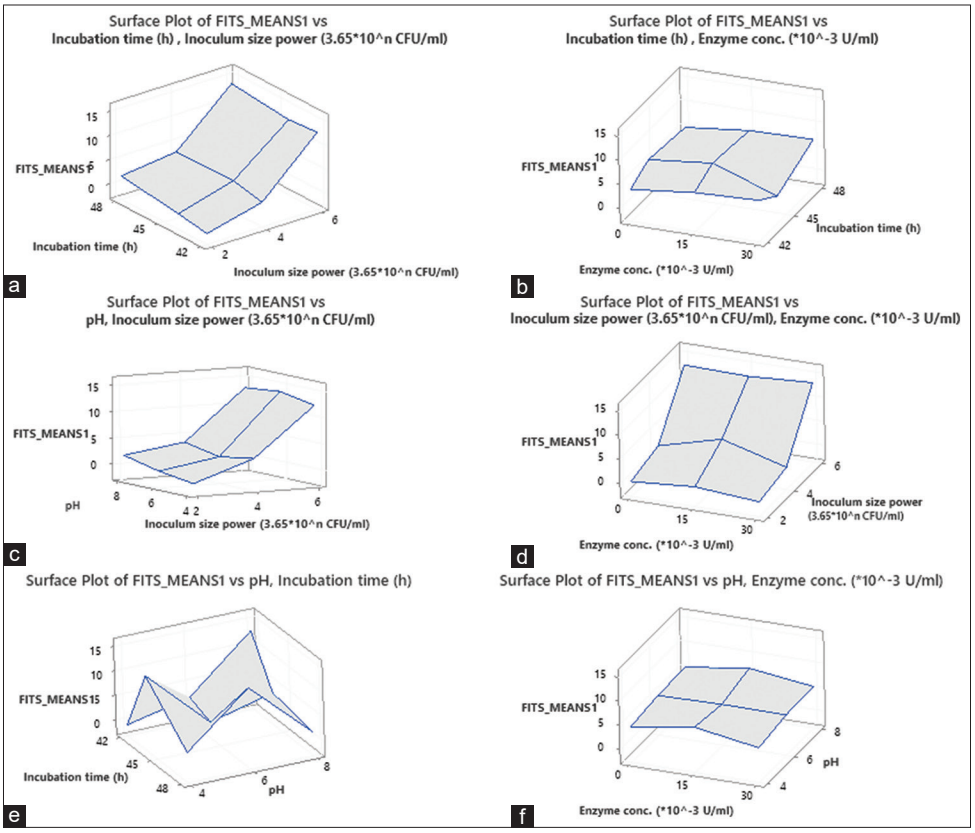

Figure 12: Surface plot of model-predicted means (FITS_MEANS1) for: (a) inoculum size power and incubation time, (b) incubation time and enzyme concentration, (c) inoculum size power and pH, (d) inoculum size power and enzyme concentration, (e) pH and inoculum size power, and (f) pH and enzyme.

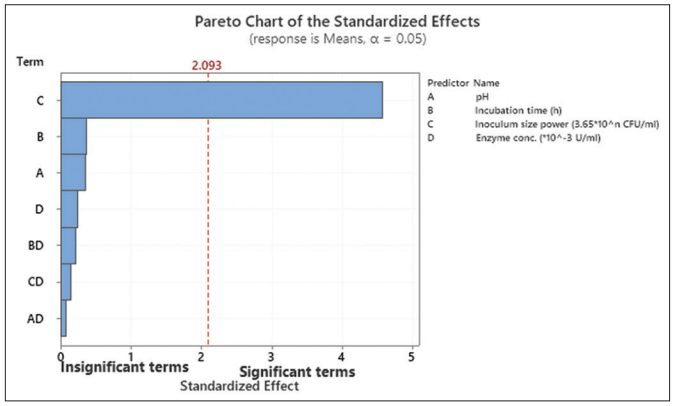

Figure 13: Pareto chart of the standardized effects, it is shown that none of the terms or their interactions has significant effect on the AChEI%, except for inoculum size power.

the effect of probiotics on improving the spatial recognition and restoring the synaptic plasticity in the animal model was previously reported [40]. Furthermore, the curative effect of *Lactobacillus plantarum* MTCC 1325 on the ACh levels, cognitive behavior, behavioral changes, and pathological hallmarks in AD-induced animal group was described. Briefly, ACh levels restored significantly in rats' brain cortex and hippocampus while the escape latency in Morris water maze significantly shortened and healthy neurons with prominent nuclei were noted. [41]. However, to our best knowledge, there are no data directly supporting the probiotics-mediated acetylcholine esterase extracellular inhibition *in vitro*.

Statistical analysis of the model concluded that, among the four studied cultivation factors, only the inoculum size had a significant effect on the AChEI%. Therefore, further room for productivity improvement could still be achieved through studying more factors, for example, cultivation media volume, media composition, presence or absence of the substrate (AChE), and temperature [42].

AChEIs production was reported from several other microorganisms. Huperzine A, with maximum activity of 75.5%, was isolated from the endophytic fungus *Alternaria brassicae* AGF041. The productivity even increased by 40.8% using multifactorial statistical approach [42]. Among 887 screened marine bacteria, 140 strains were reported to impede AChE with maximum inhibition activity of 54% for *Bacillus subtilis* M18SP4Q (ii) [27]. Many studies, additionally, indicated the presence of AChEI activity among other microbial isolates which were diligently summarized by [43], like physostigmine produced by *Streptomyces* sp. AH-4, organophosphates products from *Streptococcus antibioticus,* altenuene from *Alternaria,* and terferol from *Actinobacterial* isolate N98-1021.

5. CONCLUSION

This study was conducted to prove that probiotics could be used to mitigate Alzheimer's disease progression by blocking the action of acetylcholine esterase enzyme. In this regard, 14 isolates recorded AChEI activity, the most potent of them was identified to have 65.73% similarity to the species *Levilactobacillus brevis* and given the accession number KI271266. The potential of the isolate was optimized using Taguchi method to almost 1.7 folds of the initial activity. Therefore, this strain could be safely propagated as a promising source of AChEIs

Figure 14: Neighbor joining phylogenetic tree of the strain PI09 based on the alignment with the closest strains using maximum likelihood method and basing on internal transcribed spacer (ITS) gene Bootstrap values basing on 1000 replications are indicated at nodes. Evolutionary analyses were conducted by MEGA11 software [27].

and a pharmaceutical nutritional supplement that helps alleviating AD symptoms side by side with the chemical therapy, as a future vision isolate, characterize and quantify of the bioactive product will need, and work to better understand the probiotic inhibition activity mechanism against the enzyme, giving us a more precise understanding of the probiotic effect against AD, and its role in the gut-brain axis to be suitable for as pharmaceutical application.

6. ABBREVIATIONS

ACh: Acetyl choline, AChE: Acetyl choline esterase, AChEI: Acetyl choline esterase inhibitor, AChEI%: Acetyl choline esterase inhibition activity, AD: Alzheimer disease, ANOVA: Analysis of Variance, ATCI: Acetyl thiocholine iodide, BSA: Bovine serum albumin, CFF: Cell-free filtrate, DOE: Design of Experiment, DRS: Donepezil reference standard, DTNB: 5,5`-Dithiobis-bis-(2-nitrobenzoic acid), FTM: Fluid thioglycolate media, GRS: Galantamine reference standard, HSD post-HOC: Honest Significant Difference post-HOC, IBD: Inflammatory bowel disease, MG: Myasthenia gravis, MRS: De Man, Rogosa and Sharpe media, MSE: Mean squared error, OD: Optical density, PBS: Phosphate buffer solution, PD: Parkinson disease, RPM: Round per minute, SD: standard deviation, S/N, or SNR: Signal to noise ratio, STD: Standard, and 95% CI: 95% Confidence interval.

7. AUTHORS' CONTRIBUTIONS

All authors made substantial contributions to conception and design, acquisition of data, or analysis and interpretation of data; took part in drafting the article or revising it critically for important intellectual content; agreed to submit to the current journal; gave final approval of the version to be published; and agreed to be accountable for all aspects of the work. All the authors are eligible to be an author as per the International Committee of Medical Journal Editors (ICMJE) requirements/guidelines.

8. FUNDING

This research did not receive any grants from funding agencies in the public, commercial, or not-for-profit sectors.

9. CONFLICTS OF INTEREST

The authors report no financial or any other conflicts of interest in this work.

10. ETHICAL APPROVALS

This study does not involve experiments on animals or human subjects.

11. DATA AVAILABILITY

All data sets generated, used, or analyzed during this study are available from the corresponding author on reasonable request.

12. PUBLISHER'S NOTE

This journal remains neutral with regard to jurisdictional claims in published institutional affiliation.

REFERENCES

1. Colović MB, Krstić DZ, Lazarević-Pašti TD, Bondžić AM, Vasić VM. Acetylcholinesterase inhibitors: Pharmacology and toxicology. Curr Neuropharmacol 2013;11:315-35.
2. Kračmarová A, Drtinová L, Pohanka M. Possibility of acetylcholinesterase Overexpression in Alzheimer disease patients after therapy with acetylcholinesterase inhibitors. Acta Medica (Hradec Kralove) 2015;58:37-42.
3. Zhang HY, Tang XC. Neuroprotective effects of huperzine A: New therapeutic targets for neurodegenerative disease. Trends Pharmacol Sci 2006;27:619-25.
4. Phillips LH 2nd. The epidemiology of myasthenia gravis. Ann N Y Acad Sci 2003;998:407-12.
5. Roche P, Bouhour F. Myasthenia gravis and pregnancy. Rev Neurol (Paris) 2021;177:215-9.
6. Marucci G, Buccioni M, Ben DD, Lambertucci C, Volpini R, Amenta F. Efficacy of acetylcholinesterase inhibitors in Alzheimer's disease. Neuropharmacology 2021;190:108352.
7. Melzer N, Ruck T, Fuhr P, Gold R, Hohlfeld R, Marx A, *et al*. Clinical features, pathogenesis, and treatment of myasthenia gravis: A supplement to the Guidelines of the German Neurological Society. J Neurol 2016;263:1473-94.

8. Greathouse B, Zahra F, Brady MF. Acetylcholinesterase inhibitors toxicity. In: StatPearls. Treasure Island, FL: StatPearls Publishing; 2022.
9. Simard M, van Reekum R. The acetylcholinesterase inhibitors for treatment of cognitive and behavioral symptoms in dementia with Lewy bodies. J Neuropsychiatry Clin Neurosci 2004;16:409-25.
10. Yu P, Dong WP, Tang YB, Chen HZ, Cui YY, Bian XL. Huperzine A lowers intraocular pressure via the M3 mAChR and provides retinal neuroprotection via the M1 mAChR: A promising agent for the treatment of glaucoma. Ann Transl Med 2021;9:332.
11. Gottwald MD, Rozanski RI. Rivastigmine, a brain-region selective acetylcholinesterase inhibitor for treating Alzheimer's disease: Review and current status. Expert Opin Investig Drugs 1999;8:1673-82.
12. Tobias JD. Sugammadex: Applications in pediatric critical care. J Pediatr Intensive Care 2020;9:162-71.
13. Mörkl S, Butler MI, Holl A, Cryan JF, Dinan TG. Correction to: Probiotics and the Microbiota-gut-brain axis: Focus on psychiatry. Curr Nutr Rep 2020;9:183.
14. Woo V, Eshleman EM, Hashimoto-Hill S, Whitt J, Wu SE, Engleman L, *et al*. Commensal segmented filamentous bacteria-derived retinoic acid primes host defense to intestinal infection. Cell Host Microbe 2021;29:1744-56.e5.
15. Ming Z, Han L, Bao M, Zhu H, Qiang S, Xue S, *et al*. Living bacterial hydrogels for accelerated infected wound healing. Adv Sci (Weinh) 2021;8:e2102545.
16. Chen D, Jin D, Huang S, Wu J, Xu M, Liu T, *et al*. *Clostridium butyricum*, a butyrate-producing probiotic, inhibits intestinal tumor development through modulating Wnt signaling and gut microbiota. Cancer Lett 2020;469:456-67.
17. Wang Y, Li N, Yang JJ, Zhao DM, Chen B, Zhang GQ, *et al*. Probiotics and fructo-oligosaccharide intervention modulate the microbiota-gut brain axis to improve autism spectrum reducing also the hyper-serotonergic state and the dopamine metabolism disorder. Pharmacol Res 2020;157:104784.
18. Du R, Yu L, Yu N, Ping W, Song G, Ge J. Characterization of exopolysaccharide produced by *Levilactobacillus brevis* HDE-9 and evaluation of its potential use in dairy products. Int J Biol Macromol 2022;217:303-11.
19. Kim KT, Yang SJ, Paik HD. Probiotic properties of novel probiotic *Levilactobacillus brevis* KU15147 isolated from radish kimchi and its antioxidant and immune-enhancing activities. Food Sci Biotechnol 2021;30:257-65.
20. Jin YH, Hong JH, Lee JH, Yoon H, Pawluk AM, Yun SJ, *et al*. Lactic acid fermented green tea with *Levilactobacillus brevis* capable of producing γ-aminobutyric acid. Fermentation 2021;7:110.
21. Bock HJ, Lee NK, Paik HD. Neuroprotective effects of heat-killed *Levilactobacillus brevis* Ku15152 on H2o2-induced oxidative stress. SSRN Electron J 2022.
22. Bockwoldt JA, Fellermeier J, Steffens E, Vogel RF, Ehrmann MA. β-glucan production by *Levilactobacillus brevis* and *Pediococcus claussenii* for *in situ* enriched rye and wheat sourdough breads. Foods 2021;10:547.
23. El-Ghwas DE, Mazeed TE, El-Waseif A, Al-Zahrani HA, Almaghrabi OA, Elazzazy AM. Factorial experimental design for optimization of zinc oxide nanoparticles production. Curr Nanosci 2020;16:51-61.
24. El-Waseif AA, Roshdy TY, Abdel-Monem MO, Hassan MG. Taguchi design analysis for optimization of probiotics cholesterol assimilation. Mater Today 2022;61:1154-7.
25. De Man JC, Rogosa M, Sharpe ME. A medium for the cultivation of lactobacilli. J Appl Bacteriol 1960;23:130-5.
26. Gorun V, Proinov I, Baltescu V, Balaban G, Barzu O. Modified Ellman procedure for assay of cholinesterases in crude enzymatic preparations. Anal Biochem 1978;86:324-6.
27. Pandey S, Sree A, Sethi DP, Kumar CG, Kakollu S, Chowdhury L, *et al*. A marine sponge associated strain of *Bacillus subtilis* and other marine bacteria can produce anticholinesterase compounds. Microb Cell Fact 2014;13:24.
28. Zhao Z, Xiang Z, Haroutunian V, Buxbaum JD, Stetka B, Pasinetti GM. Insulin degrading enzyme activity selectively decreases in the hippocampal formation of cases at high risk to develop Alzheimer's disease. Neurobiol Aging 2007;28:824-30.
29. Ragab TI, Alminderej FM, El-Sayed WA, Saleh SM, Shalaby AS. Enhanced optimization of bioethanol production from palm waste using the Taguchi method. Sustainability 2021;13:13660.
30. Malhotra G, Chapadgaonkar SS. Taguchi optimization and scale up of xylanase from *Bacillus licheniformis* isolated from hot water geyser. J Genet Eng Biotechnol 2020;18:65.
31. Priyadarshi D, Paul KK. Optimisation of biodiesel production using Taguchi model. Waste Biomass Valorization 2019;10:1547-59.
32. Al-Zahrani HA, El-Waseif AA, El-Ghwas DE. Biosynthesis and evaluation of TiO2 and ZnO nanoparticles from *in vitro* stimulation of *Lactobacillus johnsonii*. J Innov Pharm Biol Sci 2018;5:16-20.
33. Saitou N, Nei M. The neighbor-joining method: A new method for reconstructing phylogenetic trees. Mol Biol Evol 1987;4:406-25.
34. Felsenstein J. Confidence limits on phylogenies: An approach using the bootstrap. Evolution 1985;39:783-91.
35. Nei M, Kumar S. Molecular Evolution and Phylogenetics. USA: Oxford University Press; 2000.
36. Tamura K, Stecher G, Kumar S. MEGA11: Molecular evolutionary genetics analysis version 11. Mol Biol Evol 2021;38:3022-7.
37. Brenner DM, Moeller MJ, Chey WD, Schoenfeld PS. The utility of probiotics in the treatment of irritable bowel syndrome: A systematic review. Am J Gastroenterol 2009;104:1033-49; quiz 1050.
38. Hamilton-Miller JM. The role of probiotics in the treatment and prevention of *Helicobacter pylori* infection. Int J Antimicrob Agents 2003;22:360-6.
39. Hendler R, Zhang Y. Probiotics in the treatment of colorectal cancer. Medicines (Basel) 2018;5:101.
40. Asl Z, Rezaei G, Sepehri M. Probiotic treatment improves the impaired spatial cognitive performance and restores synaptic plasticity in an animal model of Alzheimer's disease. Behav Brain Res 2019;376:112183.
41. Nimgampalle M, Kuna Y. Anti-Alzheimer properties of probiotic, *Lactobacillus plantarum* MTCC 1325 in Alzheimer's disease induced Albino rats. J Clin Diagn Res 2017;11:KC01-5.
42. Zaki AG, El-Shatoury EH, Ahmed AS, Al-Hagar OE. Production and enhancement of the acetylcholinesterase inhibitor, huperzine A, from an endophytic *Alternaria brassicae* AGF041. Appl Microbiol Biotechnol 2019;103:5867-78.
43. Zaki AG, El-Sayed ES, Abd Elkodous M, El-Sayyad GS. Microbial acetylcholinesterase inhibitors for Alzheimer's therapy: Recent trends on extraction, detection, irradiation-assisted production improvement and nano-structured drug delivery. Appl Microbiol Biotechnol 2020;104:4717-35.

How to cite this article:
Qadah AM, El-Waseif AA, Yehia H. Novel use of probiotic as acetylcholine esterase inhibitor and a new strategy for activity optimization as a biotherapeutic agent. J App Biol Biotech. 2023;11(6):202-215.
DOI: 10.7324/JABB.2023.141954